Supporting Information

Heterogeneous Metal Alloy Engineering: Embryonic Growth of M_{13} icosahedron in Ag-based Alloy Superatomic Nanoclusters

Ying Liu,[a,b] *Shuxin Wang,*[c] *Xi Kang,* [a,b] *Bing Yin,* [a,b] *Shan Jin,* [a,b] *Shuang Chen,**[a,b] *and Manzhou Zhu**[a,b]

a. *Department of Chemistry and Centre for Atomic Engineering of Advanced Materials, Anhui Province Key Laboratory of Chemistry for Inorganic/Organic Hybrid Functionalized Materials, Anhui University, Hefei, Anhui, 230601, China.*
Emails: chenshuang@ahu.edu.cn; zmz@ahu.edu.cn;
b. *Department Institutes of Physical Science and Information Technology, Key Laboratory of Structure and Functional Regulation of Hybrid Materials, Ministry of Education, Anhui University, Hefei, Anhui, 230601, China.*
c. *College of Materials Science and Engineering, Qingdao University of Science and Technology, Qingdao 266042, P. R. China.*

Table of Contents

Section 1. Experimental Procedures

Materials and Synthesis

Materials

Unless specified, all reagents were purchased from Sigma-Aldrich and used as received without further purification. Tetrachloroauric(III) acid ($HAuCl_4•3H_2O$, >99.99% metals basis), Chloroplatinic acid ($H_2PtCl_6•6H_2O$, >99.99% metals basis), silver nitrate ($AgNO_3$, >99%), 1-adamantanethiol (HS-Adm, >99%), Triphenylphosphine (PPh_3, >99%), sodium borohydride ($NaBH_4$, >98%), sodium hexafluoroantimonate ($NaSbF_6$, >99%), tetrabutylammonium perchlorate (TBAP, >99%), dichloromethane (DCM, HPLC grade, ≥99.9%), n-hexane (Hex, HPLC grade, ≥99.9%), methanol (MeOH, HPLC grade, ≥99.9%), ethyl acetate (EA, HPLC grade, ≥99.9%) and chloroform-d ($CDCl_3$, HPLC grade, ≥99.9%). All glassware was cleaned with aqua regia (HCl: HNO_3=3:1 V:V), and washed with copious nanopure water, then dried in an oven prior to use.

Synthesis

Preparation of Au_3Ag_{48} alloy nanoclusters. The overall synthesis process of Au_3Ag_{48} nanoclusters is directly reduce the metal complex in a mixed solvent of MeOH and EA. In a typical synthesis, 30 mg $AgNO_3$ was dissolved in 5 mL MeOH with 20 mL EA added. Then an aqueous solution of $HAuCl_4•3H_2O$ (40 μL, 0.2 mM) was added under stirring. The solution changed from white to yellow. After 5 min, HS-Adm (100 mg) and PPh_3 (100 mg) were added under vigorous stirring. The yellow turbid solution turned white after 20 minutes. 20 mg $NaBH_4$ dissolved in 1 mL nanopure water was quickly added into the solution. The reaction was allowed to overnight. To collect the crude product, the solution was centrifuged at 6000 rpm for 5 min, and the solid product was collected. The obtained material was washed with MeOH for three times. $NaSbF_6$ dissolved in MeOH was mixed with the DCM solution of product to substitute the counter ions. A mixed solvent of DCM and Hex was used for crystal growth. The synthetic yield of Au_3Ag_{48} is 15.8% on Ag mole basis. Thin layer chromatography was employed to extract the products. Pink products were collected and DCM was added to extract the Au_3Ag_{48}.

Preparation of Pt_2Ag_{51} alloy nanoclusters. The synthesis process of Pt_2Ag_{51} nanoclusters is same as that of Au_3Ag_{48} excepting for the foreign metal salt. Specially, 40 μL aqueous solution of $HAuCl_4•3H_2O$ was substituted with 50 μL aqueous solution (0.2 mM) of $H_2PtCl_6•6H_2O$. The synthetic yield of Pt_2Ag_{51} is 10.3% on Ag mole basis. Thin layer chromatography was employed to extract the products. Green products were collected and DCM was added to extract the Pt_2Ag_{51}.

Instrumentations

Electrospray ionization mass spectrometry. The crystal of Au_3Ag_{48} and Pt_2Ag_{51} are dissolved in a mixed solvent of DCM and MeOH to make a dilute solution, respectively. Then centrifuged for 5 minutes (9000 rpm) to get rid of any insoluble material. The centrifuged solution was then injected into a Bruker Q-TOF mass spectrometer at a flow rate 500 μL/min. The gas temperature was kept at 80 °C. The results are analyzed in positive ionization modes of the ESI-MS.

X-ray photoelectron spectroscopy. X-ray photoelectron spectroscopy (XPS) measurements were

performed on a Thermo ESCALAB 250, configured with a monochromated Al Ka (1486.8 eV) 150 W X-ray source, 0.5 mm circular spot size, a flood gun to counter charging effects, and an analysis chamber base pressure lower than $1x10^{-9}$ mbar; and data were collected at FAT = 20 eV.

^{31}P NMR. ^{31}P NMR data was collected on a Bruker Avance II spectrometer (400MHz). The samples was dissolved in $CDCl_3$.

Thermogravimetric analysis. Thermogravimetric analysis (TGA) was carried out on a thermogravimetric analyzer (TGA Q5000 V3.17 Build 265) with ~6 mg of Au_3Ag_{48} and Pt_2Ag_{51} in an Alumina (Al_2O_3) pan at a heating rate of 10 °C/min from room temperature to 800 °C, respectively.

UV-visible absorption spectroscopy. The UV-Vis absorption spectrum of Au_3Ag_{48} and Pt_2Ag_{51} dissolved in DCM were recorded using Agilent 8453 diode array spectrometer. The background correction was made using a DCM blank. Solid samples were dissolved in DCM to make a dilute solution, with a subsequent transformation to a 1 cm path length quartz cuvette, followed by spectral measurements.

Electrochemical measurements. The electrochemical experiments were performed on CHI 660e. A Pt disk (d=0.5 mm) was used as working electrode. A Pt foil and a Ag/AgCl wire were used as counter and reference electrodes, respectively. All data were collected at room temperature. The concentration of samples was ~15 mM with 0.1 M TBAP, and the solution was purging with argon for 10 min before experiments.

Photoluminescence spectroscopy. Photoluminescence spectra were measured on a FL-4500 spectro-fluormeter with the same optical density (OD) ~0.05. The samples were dissolved in DCM for experiment.

Single-crystal X-ray diffraction analyses. The data collection for single crystal X-ray diffraction was carried out on a Bruker D8 venture diffractometer at 296.15 K, using a Mo-K_α radiation (λ = 0.71073 Å) for Au_3Ag_{48} and Pt_2Ag_{51}. Data reduction and absorption corrections were performed using the SAINT and SADABS programs,[1] respectively. The structure was solved by direct methods (SHELXS) and refined with full-matrix least squares on F^2 using the OLEX, and the solvent was squeezed by platon, due to large solvent voids.[2,3] All the refinement parameters are summarized in Table S3 and S4.

References

[1] APEX II software suite, Bruker-AXS, 2006.

[2] SHELXTL, Sheldrick, G. M. *Acta Crystallogr.* **C 71**, 3-8 (2015).

[3] Dolomanov, O.V., Bourhis, L.J., Gildea, R.J, Howard, J.A.K. & Puschmann, H., *J. Appl. Cryst.* **42**, 339-341 (2009).

Section 2. Supplementary Figures

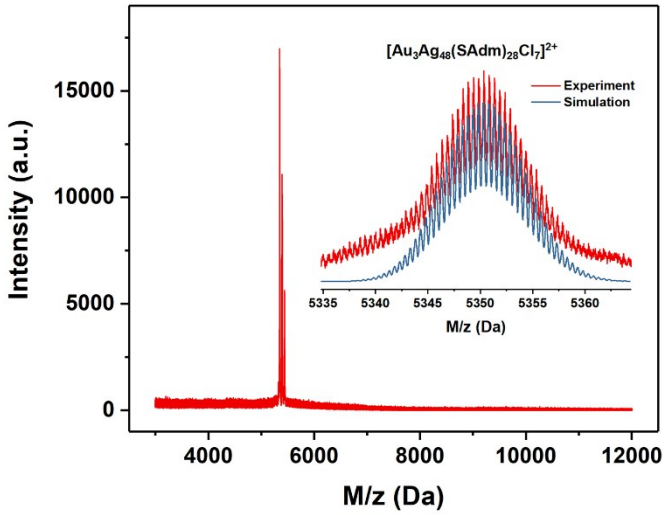

Figure S1. ESI of Au_3Ag_{48} nanoclusters. The main peak of 5350.3550 Da is assigned to the composition of $[Au_3Ag_{48}(SAdm)_{28}Cl_7]^{2+}$, which matches the simulation result.

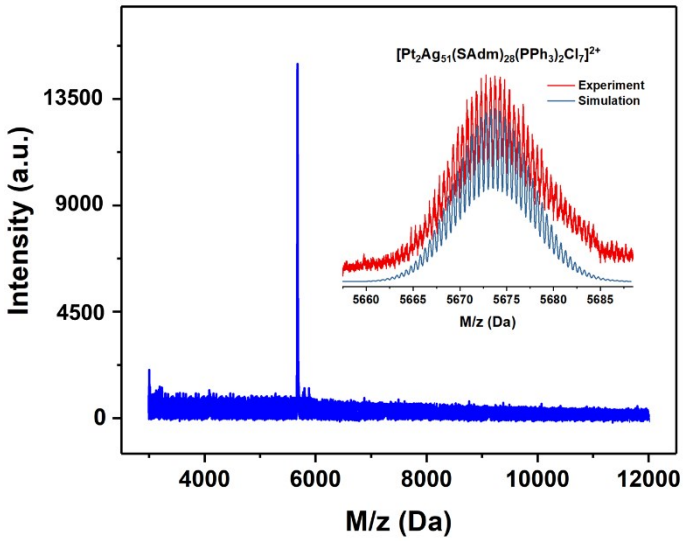

Figure S2. ESI of Pt_2Ag_{51} nanoclusters. The peak of 5673.7373 Da matches the composition of $[Pt_2Ag_{51}(SAdm)_{28}(PPh_3)_2Cl_7]^{2+}$.

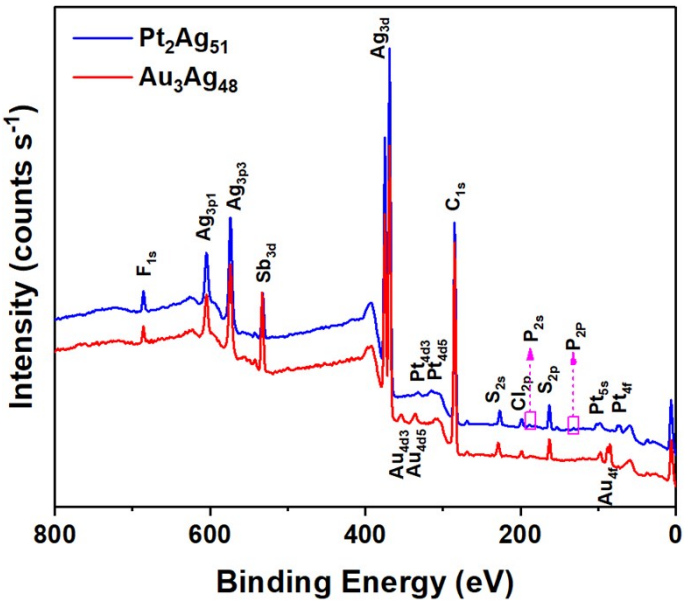

Figure S3. XPS of Au_3Ag_{48} and Pt_2Ag_{51}. P_{2s} and P_{2p} signals were merely observed in Pt_2Ag_{51}, which suggest the composition difference of Au_3Ag_{48} and Pt_2Ag_{51}.

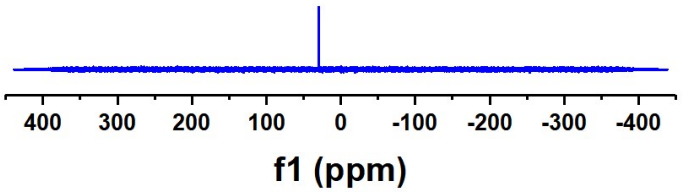

Figure S4. ^{31}P NMR spectrum of Pt_2Ag_{51}. The chemical shift of 29.8127 ppm was detected in Pt_2Ag_{51}. The only one signal indicates the same chemical environment of these two PPh_3 ligand in Pt_2Ag_{51}.

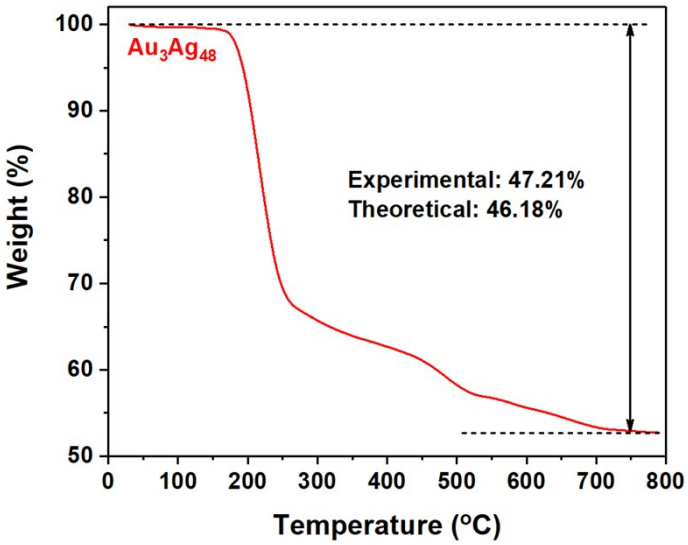

Figure S5. TGA of Au_3Ag_{48}. The experimental and theoretical weight loss of Au_3Ag_{48} are 47.21% and 46.18%.

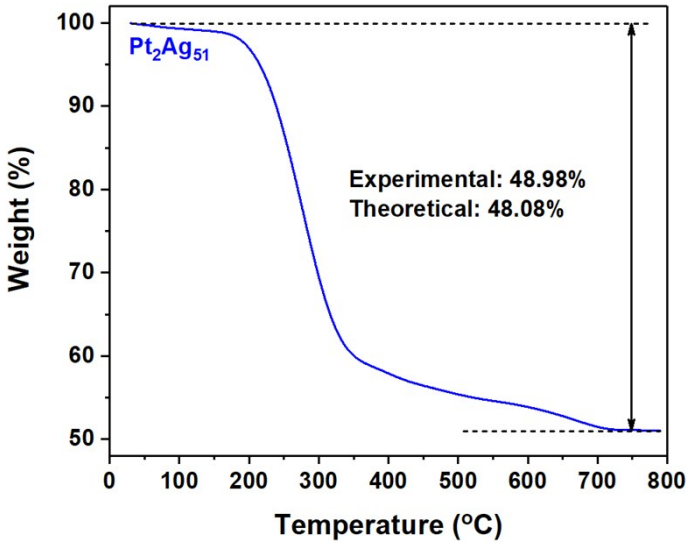

Figure S6. TGA of Pt_2Ag_{51}. The experimental and theoretical weight loss of Pt_2Ag_{51} are 48.98% and 48.08%.

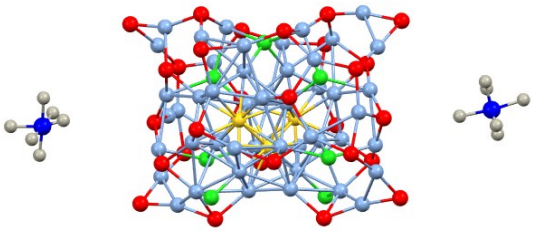

Figure S7. Total structure of $[Au_3Ag_{48}(S\text{-}Adm)_{28}Cl_7](SbF_6)_2$. All C and H atoms are omitted for clarity. Color label: pale blue = Ag; yellow =Au; red = S; green = Cl; dark blue = Sb; grey = F.

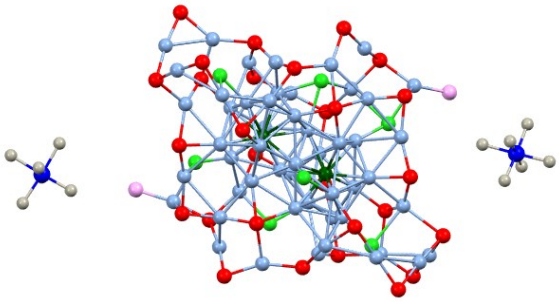

Figure S8. Total structure of $[Pt_2Ag_{51}(S\text{-}Adm)_{28}(PPh_3)_2Cl_7](SbF_6)_2$. All C and H atoms are omitted for clarity. Color label: pale blue = Ag; dark green = Pt; red = S; green = Cl; pink = P; dark blue = Sb; grey = F.

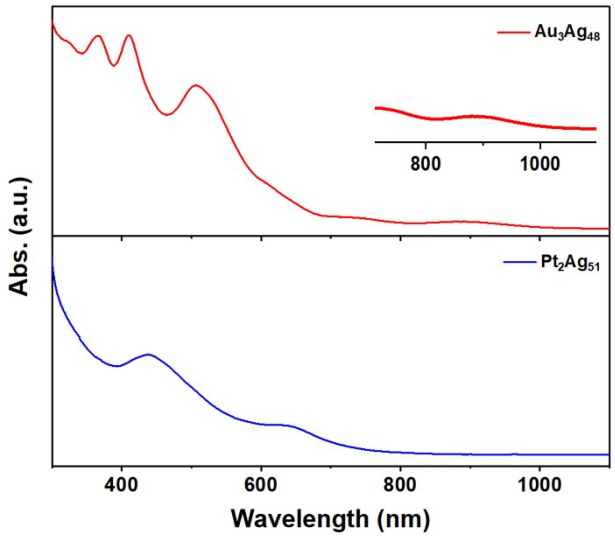

Figure S9. UV-Vis spectra of Au_3Ag_{48} and Pt_2Ag_{51}. The Au_3Ag_{48} shows multiple absorptions and Pt_2Ag_{51} shows two peaks in the UV-vis spectra.

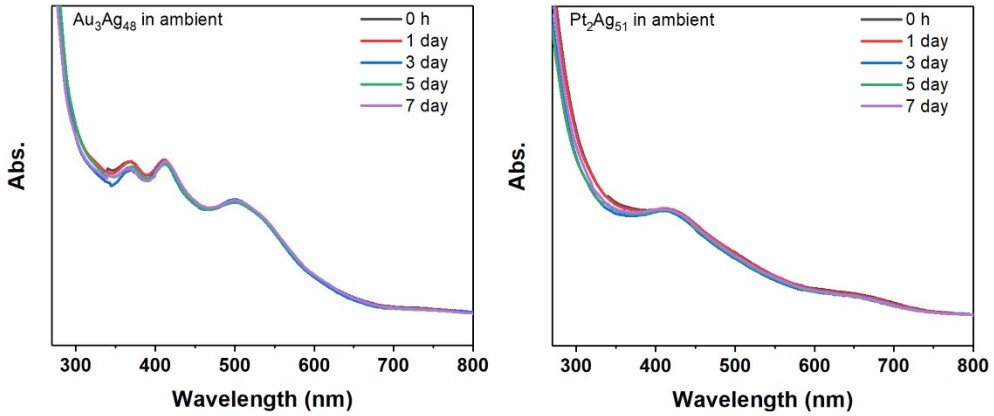

Figure S10. The UV-vis absorption spectra variation of Au_3Ag_{48} and Pt_2Ag_{51} in ambient. These two nanoclusters show good stability in ambient.

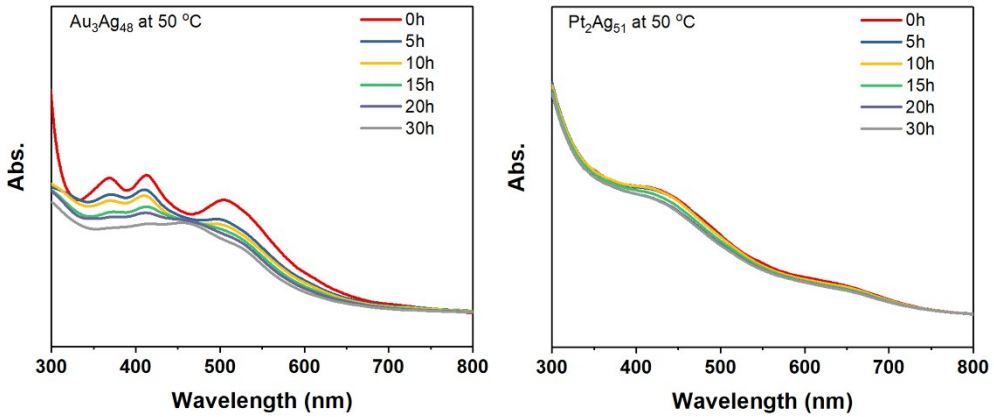

Figure S11. The UV-vis absorption spectra variation of Au_3Ag_{48} and Pt_2Ag_{51} at 50 °C. The results indicate that Pt_2Ag_{51} is more stable than Au_3Ag_{48} at high temperature.

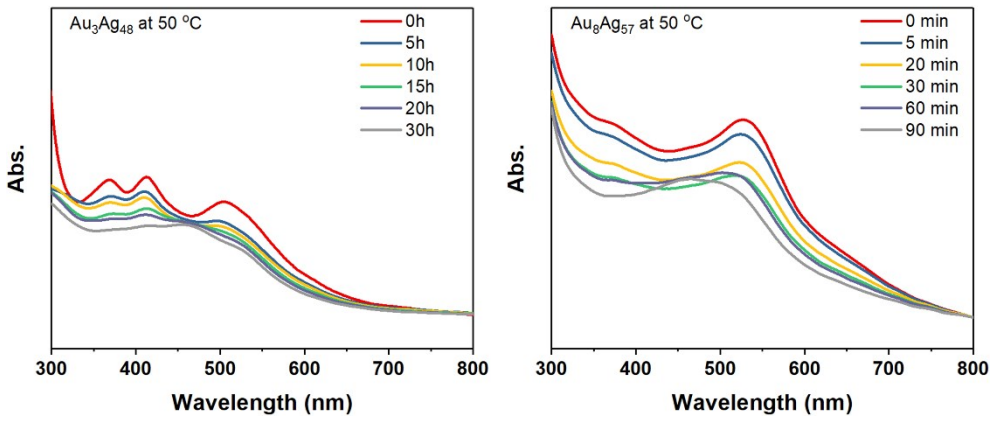

Figure S12. The UV-vis absorption spectra variation of Au_3Ag_{48} and Au_8Ag_{57} at 50 °C. The results indicate that Au_3Ag_{48} is more stable than Au_8Ag_{57} at high temperature.

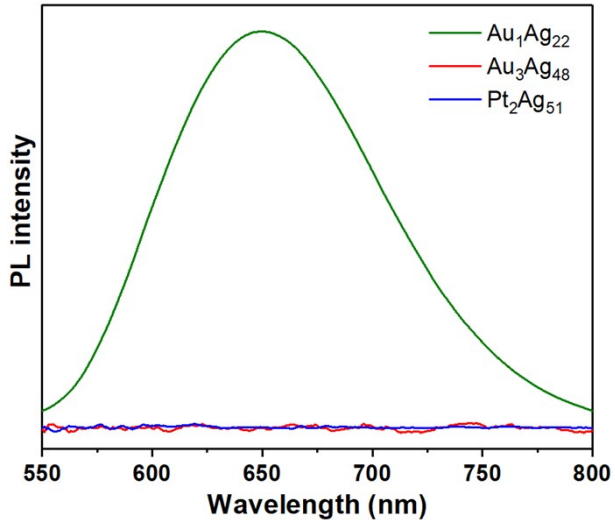

Figure S13. Photoluminescence of Au_3Ag_{48} and Pt_2Ag_{51}. The Au_1Ag_{22} with a red emission is employed as a comparison. Au_3Ag_{48} and Pt_2Ag_{51} display extremely weak and negligible emission.

Section 3. Supplementary Tables

Table S1. Atom ratio of Au and Ag in Au_3Ag_{48}.

$[Au_3Ag_{48}(S\text{-}Adm)_{28}Cl_7](SbF_6)_2$	**Au atom**	**Ag atom**
XPS Experiment Ratio	6.12%	93.88%
Theoretical Ratio	5.88%	94.12%

Table S2. Atom ratio of Pt and Ag in Pt_2Ag_{51}.

$[Pt_2Ag_{51}(S\text{-}Adm)_{28}(PPh_3)_2Cl_7](SbF_6)_2$	**Pt atom**	**Ag atom**
XPS Experiment Ratio	3.62%	96.38%
Theoretical Ratio	3.77%	96.23%

Table S3. Crystal data and structure refinement for Au_3Ag_{48}.

Identification code	Au_3Ag_{48}
Empirical formula	$C_{280}H_{406}Ag_{48}Au_3Cl_7F_{12}S_{28}Sb_2$
Formula weight	11158.01
Temperature/K	296.15
Crystal system	monoclinic
Space group	C2/c
a/Å	41.6940(5)
b/Å	29.9362(4)
c/Å	62.1774(9)
α/°	90
β/°	108.9609(6)
γ/°	90
Volume/Å3	73396.4(17)
Z	8
ρcalcg/cm3	2.020
μ/mm 1	4.087
F(000)	42848.0
Radiation	MoKα (λ = 0.71073)
2Θ range for data collection/°	2.938 to 53
Index ranges	-52 ≤ h ≤ 52, -37 ≤ k ≤ 37, -78 ≤ l ≤ 78
Reflections collected	440232
Independent reflections	76000 [Rint = 0.0981, Rsigma = 0.1114]
Data/restraints/parameters	76000/223/3746
Goodness-of-fit on F2	1.222
Final R indexes [I>=2σ (I)]	R1 = 0.1218, wR2 = 0.3289
Final R indexes [all data]	R1 = 0.1983, wR2 = 0.3725
Largest diff. peak/hole / e Å-3	11.82/-6.54

Table S4. Crystal data and structure refinement for Pt_2Ag_{51}.

Identification code	Pt_2Ag_{51}
Empirical formula	$C_{316}H_{437}Ag_{51}Cl_7F_{12}P_2Pt_2S_{28}Sb_2$
Formula weight	11806.45
Temperature/K	296.15
Crystal system	triclinic
Space group	P-1
a/Å	25.6867(13)
b/Å	30.3229(16)
c/Å	37.0200(18)
α/°	107.289(3)
β/°	99.777(3)
γ/°	110.352(3)
Volume/Å^3	24582(2)
Z	2
ρ_{calc}g/cm^3	1.595
μ/mm^{-1}	2.852
F(000)	11386.0
Radiation	MoKα (λ = 0.71073)
2Θ range for data collection/°	1.552 to 51
Index ranges	$-31 \leq h \leq 31$, $-36 \leq k \leq 36$, $-44 \leq l \leq 44$
Reflections collected	333552
Independent reflections	91119 [R_{int} = 0.1479, R_{sigma} = 0.1691]
Data/restraints/parameters	91119/393/3844
Goodness-of-fit on F^2	1.022
Final R indexes [I>=2σ (I)]	R_1 = 0.1183, wR_2 = 0.2958
Final R indexes [all data]	R_1 = 0.2222, wR_2 = 0.3502
Largest diff. peak/hole / e Å^{-3}	5.82/-5.96